

BEHAVIOR OF A STEEL STRUCTURE RAILWAY BRIDGE UNDER DYNAMIC LOADINGS

Muhammad Abi Berkah Nadi^{1*}, Wimpie Agoeng Noegroho Aspar², Willy Barasa², Suci Putri Primadiyant², Wendy Aritenang³, Meutia Nadia Karunia¹, Boy Jurdil Halawa¹

¹ Infrastructure and Regional Technology Department, Institut Teknologi Sumatera (ITERA), Indonesia

² Research Center for Transportation Technology (PR TT), National Research and Innovation Agency – BRIN, Indonesia

³ Indonesian Railway Society, Indonesia

* muhammad.nadi@si.itera.ac.id

Most old steel structure railway bridges in Indonesia have deteriorated throughout their service life since they were constructed almost a century ago. However, those bridges' performance must be maintained to have essential safety issues and live extension of the railway bridge structure. Therefore, inspecting and evaluating those steel railway bridges is necessary to maintain the service requirement. Vertical deformation of the steel railway bridge caused by dynamic loadings needs to be observed. The objective of the study is to assess the old steel railway bridge by evaluating the strength characteristics of the structures against the working forces, particularly the moving, wind, and seismic loads. In order to understand the phenomena impacted by the dynamic loadings, the steel structure railway bridge was instrumented using deformation sensors, strain gages, accelerometers, and passive infrared. The steel railway bridge was analyzed using a 3D finite element model. This study discussed the influence of dynamic loadings on the steel structure railway bridge. This paper elaborates and provides suggestions to solve problems and recommended action in practice for future study. This paper may be useful for researchers and practicing engineers.

Keywords: dynamic loadings, instrumentations, loading characteristics, natural frequency, steel railway bridges, vertical deformation

1 INTRODUCTION

Steel railway bridges were constructed in conjunction with the construction of railway lines in Indonesia. Many steel structure railway bridges were built almost a century years ago. In recent years, steel railway bridge loading conditions have been adjusted due to the increase in freight volumes [1]. Furthermore, to maintain essential safety issues and the steel railway bridge life extension, it is necessary to rehabilitate the bridge to some degree. In addition, many of the old steel structure railway bridges have experienced gradual deficiencies over time and are finally deteriorating structurally.

Load testing is a common practice and valuable evaluation of steel railway bridges. This practice provides related information regarding bridge capacity when insufficient. Load testing method can be performed to evaluate existing steel structure railway bridges when the bridges are in operation. Many existing steel railway bridges have passed the design life. Many existing steel railway bridges sometimes received loads more significant than the loads during the design period. Load testing was applied on steel structure railway bridges to monitor the level of bridge damage to assess the work of the existing railway bridge [2].

Dynamic loading on a railway bridge is a significant parameter of infrastructures during post-construction maintenance. The structural performance of bridges damaged by moving loads or deficient existing bridges is becoming increasingly crucial for evaluation and inspection. In order to deal with this condition, it is necessary to have a monitoring system that can automatically detect the behavior of structural anomalies. The development of damage detection techniques can be applied to monitor whether the structure's service life has exceeded the design limit. When long-term monitoring of bridges is required, instrumentations are usually installed to determine the frequency of the railway bridge [3],[4]. Damage detection technique for bridge structure under moving vehicle loads was evaluated numerically and verified experimentally [5]. However, field measurements using instrumentation sensors are necessary for actual investigation. The sensors that can monitor the vibration due to loading on the bridge are in the form of an accelerometer. An accelerometer is a sensor that can measure acceleration and detect and measure vibrations [6].

It is necessary to maintain service and performance by evaluating the steel structure of railway bridge conditions. The steel railway bridge evaluation is necessary when significant deviations from the technical description are found, some damages are observed, and the railway bridge exceeds its planned service life. Finite element analysis was commonly applied to simulate numerically and calculate analytically for the railway bridge assessment [7].

The structural health monitoring technique is necessary to evaluate bridge structure instead of only performing a visual inspection. Construction or structural defects may cause an infrastructure failure due to working dynamic loadings. Therefore, the reliability and durability of steel structure railway bridges regularly have to be monitored [8].

The loading combinations of the dynamic moving load and the static load result in additional vertical deformation of the rail structure. For this reason, it is necessary to routinely maintain steel structure railway bridges to extend the service life of steel railway bridges. Nonetheless, regular maintenance is always viewed as an expense-consuming

railway activities. Meanwhile, competition in the traffic market demands repair and maintenance. Regular maintenance actually aims to maintain safe operation while saving maintenance costs [9].

The physical characteristics of the steel railway bridges may change when the bridge structure is damaged. This structural change will cause structural parameters to change. The typical real-time response to the bridge stiffness is the dynamic deflection of the steel railway bridge. This phenomenon can be identified and analyzed using the dynamic equation to the bridge-vehicle interaction system [10]. The structural health monitoring system can be used to evaluate the steel railway bridge's integrity and serviceability. This system determines the position and damage level of the steel railway bridge. In addition, the steel railway bridge load-carrying capacity based on the given damaged components can numerically be calculated [11]. Assessment and prediction of high-speed railway bridge long-term deformation based on track geometry inspection big data was introduced by analyzing approach for assessment and prediction of railway bridge deformation [12].

Improvement and inspection of the steel structure railway bridge condition to achieve the steel railway bridge serviceability are mandatory. Therefore, in order to know the vertical deformation that occurs due to dynamic loadings, this effort is aimed to evaluate the steel structure railway bridge strength due to working loads, particularly the moving and seismic loads.

2 MATERIALS AND METHODS

2.1 Description and Case Study Overview

The case study of the railway bridge is a steel structure railway bridge. The steel railway bridge was constructed almost a hundred years ago, and it was reconstructed in 1997. The research activity of the study was to study the existing steel structure railway bridge. Vertical deformation of a railway bridge due to dynamic loading was assessed. The bridge is a steel structure with 61.60 meters in span length. It is a one-lane railway bridge and seats on wooden sleepers. The Warren type configuration of the steel railway bridge is an 8.00 meters vertical height and a 61.60 meters single span, with a width of 4.80 meters, respectively. Fig. 1 illustrates the longitudinal concept of the railway bridge, the cross-sectional perspective, and its surrounding.



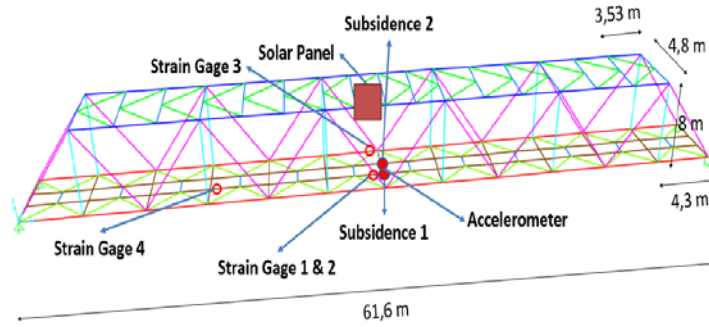
Fig. 1. The steel structure railway bridge perspective of the case study

This railway bridge is passed by coal transport trains every day. The average frequency of these coal-carrying trains is 46 times per day. Each series of coal-carrying trains usually requires two or three locomotives to move the series of trains because of the length and weight of the cargo transported. Once operating, this train consists of a super series of 60 carriages. Degradation has gradually occurred to the steel railway bridge over time.

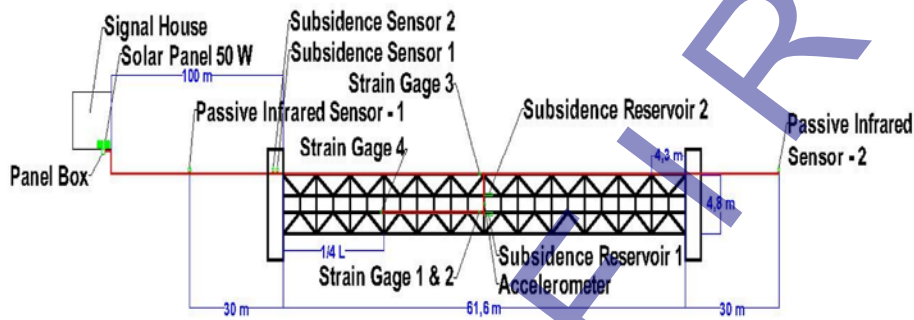
In this study, the steel structure railway bridge was 3D modeled in detail, and the numerical analysis was done using finite element analysis. Finite element analysis was carried out using SAP2000® Ver software. 6.113 [13]. Subsequently, the railway bridge was modeled and analyzed numerically. Due to incomplete documentation, therefore, the structural steel profiles were directly measured at the site to double-check geometric measurements [14].

2.2 Equipment and Instrumentations

The railway bridge was instrumented using subsidence sensors, strain gages, accelerometers, and passive infrared. The purpose of the railway bridge instrumentations was to evaluate and monitor vertical displacement, the stress distribution of the structure members, and vibration magnitudes due to a combination of loads working on the steel railway bridge. The loading combination criteria followed the applicable code of standard for the steel railway bridge structure [15]. The schematic instrumentation locations of the typical open-web girder, as presented by Barasa [16] are illustrated in Fig. 2.



(a) Schematic perspective view of instrumentation locations on the railway bridge



(b) Schematic bottom view of instrumentation location

Fig. 2. The schematic instrumentation location

Subsidence sensors monitored vertical displacement impacted by loading combinations. Vertical displacement at the center of the span is monitored for all two main girders as well. A displacement sensor is installed for this measurement. Using a hydraulic pressure system, a linear subsidence sensor is used as a displacement sensor. The degree of viscosity of the liquid greatly influences the hydraulic pressure used to measure deflection. One of the most important factors is the vertical displacement at midspan, which indicates the maximum deformation and overall stiffness of the bridge. All main beams in the mid-span have displacement measurement equipment installed.

The strain gages were mounted on the bridge's main girder (outer side) and pasted in the middle of the lower wing of the profile. In addition, the strain gages were also mounted on a stringer and affixed to the center of the lower wing of the profile. The strain gages were used to monitor the stress distribution of the railway bridge structure. These could indirectly also identify the long-term deflection of the bridge due to the possible shrinkage strain.

The accelerometers were used to determine the magnitude of the frequency that occurs on the bridge with the ability to read movement in 3 directions, namely the X, Y, and Z axes, respectively. These accelerometer sensors were placed in a single circuit called a mod bus. The positions were in the middle of the railway bridge. The instrumentation scheme for a typical open-web girder is shown in Fig. 3.

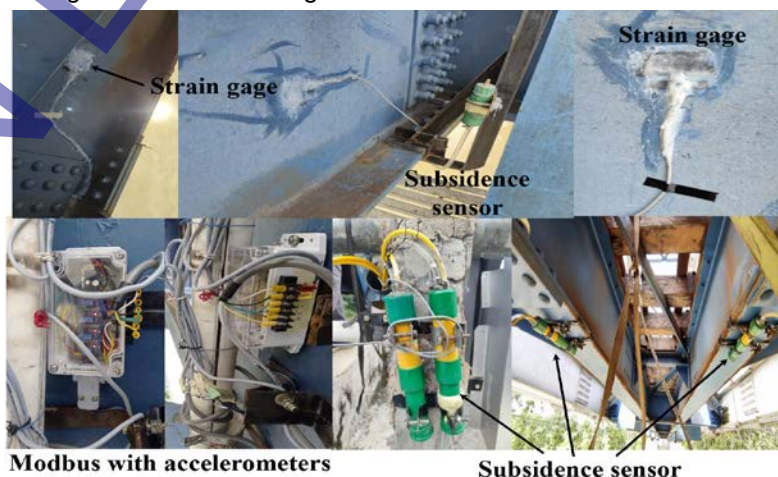


Fig. 3. Placement of subsidence sensors, mod bus with accelerometers, pressure transducer and strain gages



Fig. 4. Location of passive infrared sensors relative to the steel structure railway bridge

Passive infrared are sensors that indicate that the train is crossing the railway bridge. Therefore, passive infrared is installed in two different locations, namely at both ends of the bridge before and after crossing the railway bridge. The placement of the passive infrared sensors is shown in Fig. 4. Data recording is carried out when the train passes through the steel railway bridge and at a six-minute interval.

2.3 Data Acquisition Techniques

Sensors were used to measure dynamic loadings and direction, vibration, strain, and vertical displacement based on parameters in structural health monitoring of the steel railway bridge. One of the aspects that can cause deterioration to the bridge structure is vibration due to the load from the train passing on the bridge. Therefore, the vibrations caused by moving load, wind load, or seismic activity should be monitored using sensors. When long-term monitoring of bridges is required, sensitive instrumentation measurement is usually installed to determine the components of the bridge frequency [3],[17],[18].

The data acquisition sensors are installed in the main girder in order to be able to upload the data to the data logger. The data logger is placed at a safe location in a signal house, as shown in Fig. 6. A signal generated by the instrumentation sensors is then forwarded through the microcontroller and can then be read on a computer. Data acquisition techniques include the data recording technique passing through sensor systems of vertical displacement, the stress distribution of the steel railway bridge, and vibrations.



Fig. 5. Locations of data loggers at site

Measurement data collected from instrumentation sensors are gathered and saved into Cloud Storage as a gateway database system. The collected data are transferred to the command center via a cloud data center and virtual private network. By providing information resources to the data center, the programs are set based on the need to obtain intelligent control monitoring parameters. A steel bridge health monitoring technique was established according to the saved data set on the cloud storage that can be used in the near future [11].

For monitoring purposes, all instrumentation sensors are connected to the data logger. The transferred data will enter the document control via the data interface. Therefore, analysis can be done automatically using the expert system located in the control room in the office center. This expert system can be adapted for other civil engineering purposes [19]. An expert system would be developed by using the big data set during the application of SHMS on the steel railway bridge of this study.

2.4 The Railway Bridge Finite Element Model

The detailed descriptions for employing the numerical analysis of the framework for the truss railway bridge are elaborated by implementing a finite element technique of the steel railway bridge. The steel railway bridge was modeled and analyzed using the finite element software application described in advance. The three-dimensional numerical model of the steel railway bridge was developed and calculated numerically. The finite element model of the steel railway bridge is illustrated in Fig. 6.

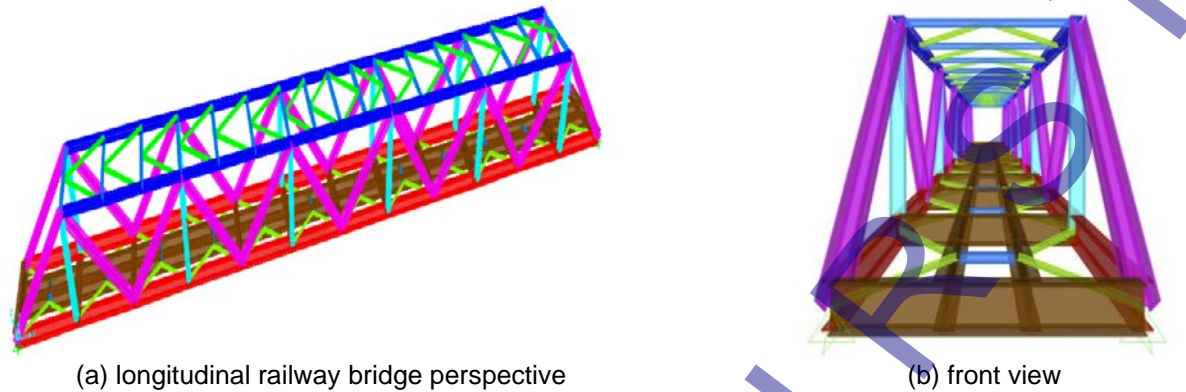


Fig. 6. Finite element model of the steel structure railway bridge

According to shop drawings and material properties, the three-dimensional numerical model of the steel railway bridge was established in the SAP2000 software package. Geometric dimensions were adjusted according to field observation and measurements. The structural model composes of beam elements representing the structural railway bridge members. The material properties of the steel components were assumed as specified in the design plans. The material properties adopted for numerical simulations were quality material grade BJ55 steel, an elasticity modulus of 200,000 MPa, and yield stress of 240 MPa (ST37), respectively. The adjustment was made to justify inspection and observation results in the location due to the lack of information.

In the numerical analysis, the abutment steel railway bridge end is supported by hinges. Rollers support the other pier end. This assumption considered that both supports are smooth without frictional resistance to ensure only translational restraint. There is no rotational restraint that is permitted at the booth ends. The model assumptions of the steel railway truss bridge analyzed in this way were also carried out by Azim and Gül in developing a model for the detection of damage to the steel railway bridge structures [20],[21].

The steel railway bridge model established in this study is a steel structure with 61.60 meters in single span length deck type girder. The steel railway bridge composes of two main girders with the type of H 700x300x48x30. It is a single-lane railway bridge and seating on wooden sleepers. The steel railway bridge width is 4.80 meters center-to-center between the two main girders, and a vertical height is 8.00 meters. The railway truss bridge is a Warren configuration consisting of H350x450x35x22 section diagonals. The railway steel bridge structure is braced using H125x125x10x10 on top of the bridge and 2L125x125x10x10 underneath sleepers.

3 RESULTS AND DISCUSSION

3.1 Loading Characteristics of the Railway Bridge

The symmetrically distributed load was applied by evenly combining the dead and the moving loads. This simulation was done to understand that the deformation and stresses found were similar. The resulting loading combinations should be smaller than the applicable standard [22]. It is better to simulate simpler numerical modeling before applying a complex numerical technique under the proposed combination of loadings. This was performed by synchronizing all the steel railway bridge geometries in order to have completely symmetrical and uniform bridge conditions.

The load-carrying capacity requires identifying a critical condition of construction members with the lowest strength value in the railway bridge. Furthermore, existing bridge elements shall exhibit reliable load-carrying capacities. Therefore, a variety of load combinations were applied to the structure at the same time. If that is the case, the usual structure design recognizes that it is unlikely that the maximum values of loads will not be applied concurrently to the structure.

One of the aspects that can cause damage to the bridge structure is vibration due to the dynamic load from the train passing on the bridge as well as seismic activity. Therefore, the vibrations caused by dynamic loadings must be monitored using sensors. The sensors that can monitor the vibration due to dynamic loadings on the bridge are in the form of an accelerometer. Three directions (X, Y, and Z) of vibration measurements on the railway bridge were also recorded by the accelerometer sensors. The accelerometer sensor data for the X, Y, and Z axes are 10.47 mG, -2.09 mG, and 30.31 mG, respectively. Fig. 7 displays the frequency that accelerometers produce. Fig. 7 indicates that the maximum frequency reported by the accelerometer sensor is in the direction of the Z axis. This phenomenon happens as a result of the Z axis direction vibration having the greatest vertical deflection.

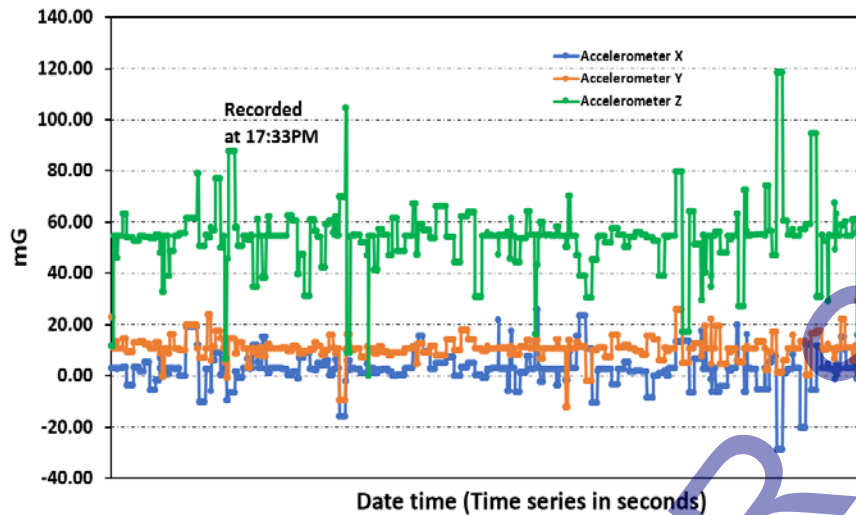
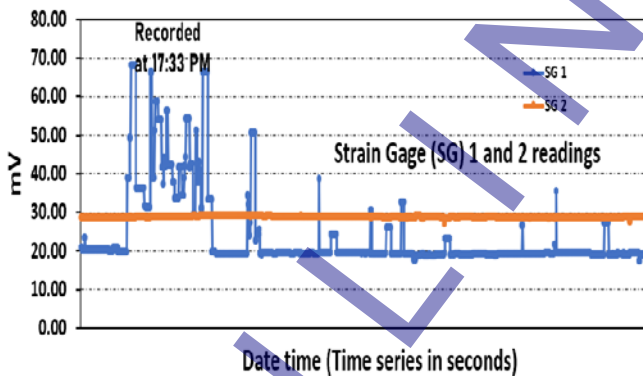


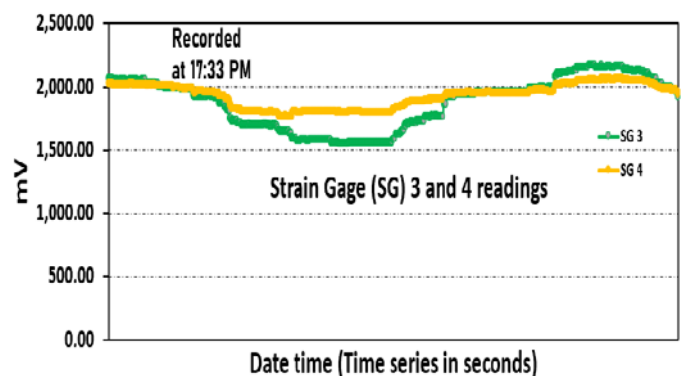
Fig. 7. Results of accelerometer sensor readings

Additionally, readings of the tension at four distinct points on the railway bridge were recorded by means of the strain gage sensors. According to the sensor data, the values for strain gages one to four are, in order, 18.91 mV, 28.78 mV, 1,943.06 mV, and 1,962.34 mV. The voltage differential that existed at locations 1 to 4 was not significantly different, according to the outcomes of numerical simulations. Nevertheless, as Fig. 8 illustrates, there was a highly notable deviation from the sensor measurement results, specifically from the sensor values for strain gages 1 and 2 with 3 and 4. This happens as a result of the implementation method's changing of the amplifier settings for strain gages 3 and 4.

There are many factors affecting the railway bridge structure under dynamic loads. It was considered difficult to analyze these parameters in analytical calculation [23],[24]. Wind load also contributes a very critical parameter of dynamic analyses. In order to overcome this factor, a wind load modeling method was proposed concerning a train traveling at high speed [25],[26]. Examination regarding the wind load influence on the footbridge structure of an untypical structure was carried out by assuming lateral wind pressure [27]. Varying dynamic loads could also affect the deformation of a simply supported railway bridge [28],[29]. Bearing these factors in mind, therefore, the moving loads (ML) model describing a load as a set of concentrated forces moving at a constant speed was considered during numerical analysis.



(a)



(b)

Fig. 8. Results of strain gage sensor measurements

3.2 Bridge Deformation Assessment

The deformation of the railway bridge was numerically analyzed. The deflection of the railway bridge in the field was confirmed using the subsidence sensors positioned as in Fig. 3. Deflection was calculated at the middle span of the steel railway bridge using the method discussed in the previous section. This bridge deformation assessment was carried out on a steel frame railway bridge due to the loading of three types of trains which were considered to frequently cross the railway bridge. The three types of trains are passenger trains, freight trains and coal trains. Coal trains are often also called Babaranjang trains, which means a long series of coal trains. Coal trains (Babaranjang trains) often require two or three locomotives to pull and push the coal train series when the coal train is fully loaded. The maximum deflection calculated numerically for the three types of trains is presented in Fig. 9. The measured deformation is plotted against the dynamic increasing moving loads.

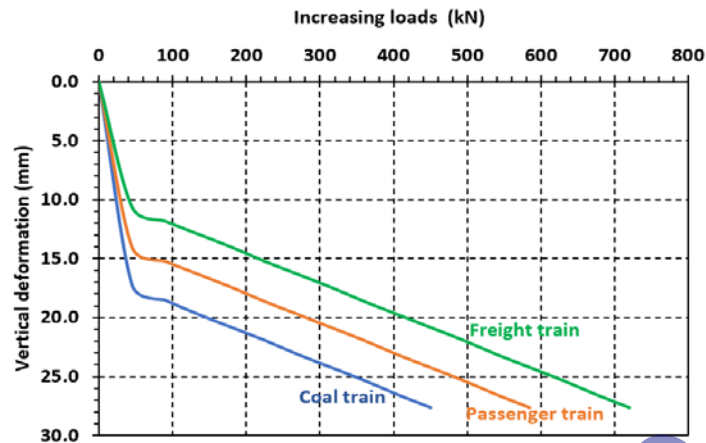


Fig. 9. Numerical simulation results of the maximum deformation of the steel railway bridge under dynamic loads

The maximum deflection under critical moving loads calculated was 27.60 mm. The maximum deflection achieved due to the increase in the dynamic moving loads of the coal train (Babaranjang train), passenger and freight trains is 450 kN, 585 kN, and 720 kN, respectively. It can be observed that the most critical deformation of the railway bridge is when the coal train passes over the railway bridge. It is true because coal-carrying trains usually require two or three locomotives to move the series of trains. This is due to the length and weight of the cargo transported. Maximum deflection occurs when the increasing dynamic load of the coal train reaches a load of 450 kN. While the same maximum deflection occurs due to the increasing dynamic moving loads of freight trains reaching a load of 720 kN. This indicates that freight trains do not significantly impact the steel railway bridge failure. However, the three types of trains crossing the railway bridge show the same deformation tendency.

The maximum displacement sensor was observed from the results of the field measurements for a period of one month on the pressure transducer sensors. It can be observed from Fig. 10 that the maximum deflection of the displacement sensor that occurs after filtering the data produced a value of 0.100 m (100.81 mm) and -0.111 m (111.43 mm). The railway bridge experienced maximum deflection when the two serial locomotives of the Babaranjang coal train just passing over the bridge. It was recorded at 17:27 PM Indonesia western time. The most vertical deformation took place at the mid-span railway bridge collected by subsidence sensors with respect to the reference time. However, the average deflections during one day were 19.81 mm and -27.54 mm. Based on Regulation of the Minister of Transportation of the Republic of Indonesia Number 60 of 2012, from the measurement results, it is found that there are a lot of deflection data that exceed these provisions, with the result that the data were limited up to $L/1000$ which means 61.6 mm, and data above the limit considered an anomaly. When the two coal train serial locomotives were slightly above the railway bridge, there was the greatest deflection took place. The results of the numerical analysis are comparable to the field monitoring and assessment of the displacement phenomenon. The baseline computation and analysis were followed for analyzing the displacement sensor results. After calculating the most recent baseline data from the displacement data collected when the train crossed the bridge, the displacement values were calculated. When the train failed to pass the midspan railway bridge, the data gathered by subsidence sensors was deemed to have been altered into a vertical deformation relative to the reference time, and the displacement value of the railway bridge was deemed to be equal to zero. It is clear that the outcomes of the numerical analysis and field observation and assessment of the displacement phenomenon are consistent. The railway bridge's deflection readings were notably lower than those of the standard criterion.

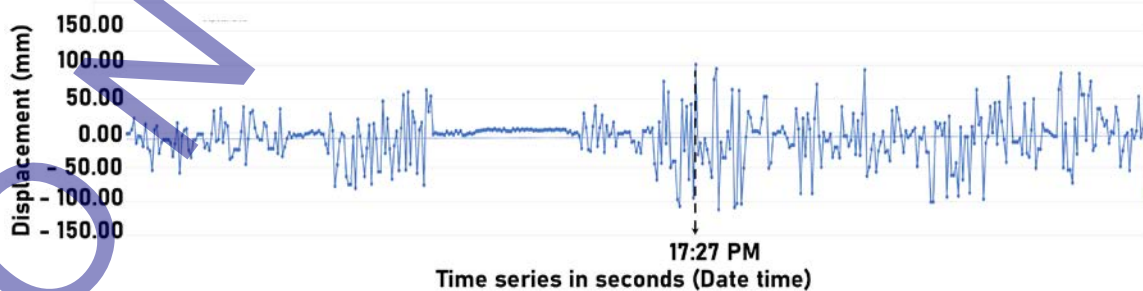


Fig. 10. Measured displacement data of sensor readings with respect to the reference time

The railway bridge was modeled using two load schemes, by considering a combination of dead load plus live load simultaneously resulted in a 41.925 mm (0.0419 m) maximum deflection and static load scheme with additional load such as traction load, wind load, impact load and lateral force, produced vertical deflection of -98.088 mm (0.098 m) [9],[16]. This maximum vertical deformation is smaller than that generated by the full strong loading combination (dead load, live load, impact load, and lateral force). Therefore, the railway bridge deformation characteristics showed significantly less than field measurements. However, before the railway bridge collapses, maintenance must be carried out by the bridge owner to ensure that the bridge can carry larger rail loads. In this case, the existing geometric

measurement data obtained from the bridge structure is necessary for structural assessment and maintenance procedure [30]. The results of this study confirm that the steel railway bridge has sufficient capability to support heavier dynamic moving loads.

3.3 Threshold Estimation Indicator

Determination of the estimated threshold is needed to evaluate the safety threshold of the bridge structure. Specifically, the threshold criteria developed are based on three selected outputs, namely deflection, stress, and natural frequency. These three parameters will later be integrated into a single sustainable threshold unit. The deflection in this case study is set at a maximum of 61.6 mm based on the Regulation of the Minister of Transportation of the Republic of Indonesia Number 60 of 2012 [15], which states that the maximum deflection that occurs in steel frame railway bridges is $L/1.000$, where L is the length of the bridge span. Based on the consideration of bridge age which is commonly used and referred to as SNI 1729:2015 [31], the allowable stress should be reduced so that it becomes 70% of the yield stress value (f_y). The yield stress (f_y) of the steel used for the railway bridge is 240 MPa (ST 37) – EN code 10002, so the maximum allowable stress is 168 MPa.

Based on EN 1991-2:2003 [32], there is a determination of the lower limit and upper limit of the natural frequency by classifying two bridge span criteria, namely the bridge span between 4 meters $\leq L \leq 20$ meters (Criterion I) and 20 meters $< L \leq 100$ meters (criterion II). In classifying this criterion, the railway bridge has a span of 61.6 meters, so determining of the upper and lower limits follows criterion II. Based on the lower and upper limits of the natural frequency therefore, the natural frequency of the steel railway bridge under study is $3.58L^{-0.592} = 2.056$ Hz and $94.76L^{0.748} = 4.345$ Hz, respectively.

Azim and Gül (2019) [17] defined that threshold indication is determined by comparing acceleration response to the train series motion obtained from the baseline bridge's threshold before any damage. The responses were obtained at a frequency of 200 Hz. This response was observed when the train passed at a speed of 50 km/h with an additional one car to the original configuration. The damping ratio was kept constant at 1%. Experimental proof indicated that the decrease in girder thickness caused potential damage features that might take place. The damage features were clearer as the values increased over threshold [33]. Damage features are obtained by increasing the speed of the train. The simulation was carried out 200 times; when damage features cross over the baseline subsequently the damage could occur [34].

In this study, the determination of the safety level of the bridge is categorized into three safety scales specific to the bridge's superstructure. Scales 1, 2, and 3 indicate that the bridge is in safe, alert, and unsafe conditions based on a combination of parameters among deflection, stress, and natural frequency displayed in the dashboard readings sent from field sensor data. Identifying scales 1, 2, and 3 only shows that the three outputs in question exceed the predetermined safety threshold. Other conditions that would be added to the safety scale of the railway bridge, such as changing the shape of the bridge from the existing visual condition, can be inspected in advance. The grouping of bridge safety scales can be used as a basis for determining the steps that must be taken, such as inspection or structural reinforcement, when sensor measurement results indicate the strength of the bridge structure in an unsafe condition. The greater the number of scales, the more detailed the condition of the bridge structure at that time.

The determination of the steel railway bridge safety scale in this study based on the safety threshold can be seen in Table 1. The scale reading on the dashboard is based on the value read by the sensor in the field. If one of the three criteria has the greatest value, the final scale combination refers to the largest scale or the most critical condition. Another important note is that when the dashboard shows a scale of 2, be alert. It is necessary to carry out a field inspection in accordance with applicable provisions to find out whether there are structural changes or damage to the bridge.

Table 1. Steel railway bridge safety scale of the object study

Parameters \ Scale	1	2	3	Threshold
Deflection (mm)	0 – 55.40	55.41 – 59.75	> 59.76	61.60 [15]
	0 – 90%	91 – 97%	> 98%	
Stress (MPa)	0 – 151.20	151.21 – 162.96	> 162.97	168 [31]
	0 – 90%	91 – 97%	> 98	
Upper limit frequency (Hz)	3.201 – 4.231	4.232 – 4.311	> 4.312	4.345 [32]
	0 – 90%	91 – 97%	> 98%	
Lower limit frequency (Hz)	3.201 – 2.171	2.170 – 2.09	< 2.09	2.056 [32]
	0 – 90%	91 – 97%	> 98%	

The first step in determining the safety scale of the steel frame railway bridge in this study is to set the threshold of each yield parameter such as deflection, stress, and natural frequency in accordance with applicable provisions, regulations, and standards. The determination of the threshold is referred to from several references based on the determination of the parameters. The deflection parameter is taken in accordance with the Regulation of the Minister of Transportation of the Republic of Indonesia Number 60 of 2012 [15]. The limiting stress that occurs on the steel railway bridge is determined by considering the estimated age of the steel railway bridge, which is commonly used

and referred to as SNI 1729:2015 [31]. Natural frequency is set into two threshold limits, namely the upper limit and lower limit, according to the provisions of EN 1991-2:2003 [32].

The percentage value of the deflection and stress parameters is determined based on the maximum value from the numerical simulation results and is adjusted to the amount of load that passes on the railway bridge. The same applies to the percentage of natural frequency parameters but is distinguished in 2 conditions, namely the upper limit and lower limit. The scale of 1 of the natural frequency is the safest range of values between the upper and lower limits. For the upper limit, the higher the result value of the parameter, the declared unsafe. The same applies to the lower limit, i.e., the lower the result value of the parameter, the declared unsafe.

3.4 Failure and Damage Identification

Case damage analysis can indicate the proposed damage detection criteria to ensure data validity. The damage case is analyzed by lowering the magnitude of the truss elements' elasticity modulus. This truss element modulus is representative of the stiffness decrease along structural elements. This damage identification takes place slowly. Therefore, this damage indication is appropriate for initial evaluation before complete failure. Modulus of elasticity might decrease structural stiffness and load-carrying capacity of the steel structure railway bridges [11],[35]. Damage detection can be identified by combining analysis of acceleration and strain responses [20]. The failure could be verified experimentally by simulating the moving load applied to the bridge structures using the delay vector variance method [5].

In addition, failure is detected when the stress ratio of the railway structure passes the value of one. The stress ratio is the ratio of stresses that occur due to an increase in dynamic loads to the stresses of the existing structure in the initial conditions under the load of the structure's own weight. Failures can be verified numerically by simulating a dynamic moving load applied to the steel structure railway bridge. Dynamic moving loads were numerically calculated by adding incrementally to the load on the coal trains (Babaranjang trains), passenger trains, and freight trains. Due to the addition of moving loads on the bridge, it is indicated that the bridge may fail when the stress ratio exceeds one. Fig. 11 shows that the coal train (Babaranjang train) is the train with the most critical tendency to cause failure. When the additional load on the coal train (Babaranjang train) reaches 400 kN, the railway bridge is indicated to have failed. Meanwhile, freight trains start showing the railway bridge failure when the additional moving load reaches 675 kN. This gives the impression that freight trains are not as critical as the coal train (Babaranjang trains). Therefore, the installation of a weight-in motion measuring device on a railway bridge is highly recommended for early detection of the possibility of a failure on a railway bridge.

The effect of environmental condition changes could influence strain data. Temperature changes could alter the physical properties and vibration response of the steel railway bridges [36]. Temperature influence should be avoided during the damage detection process. A damage detection approach based on auto-associative neural networks was proposed to detect the structural damage in bridges by eliminating the temperature effects [37]. In this study, temperature changes did not have a significant effect. This is because the difference between the maximum and lowest temperature changes throughout the year is relatively small and does not cause any differences. Thus, eliminating the effect of temperature does not affect the response of the physical properties of the railway bridge structure.

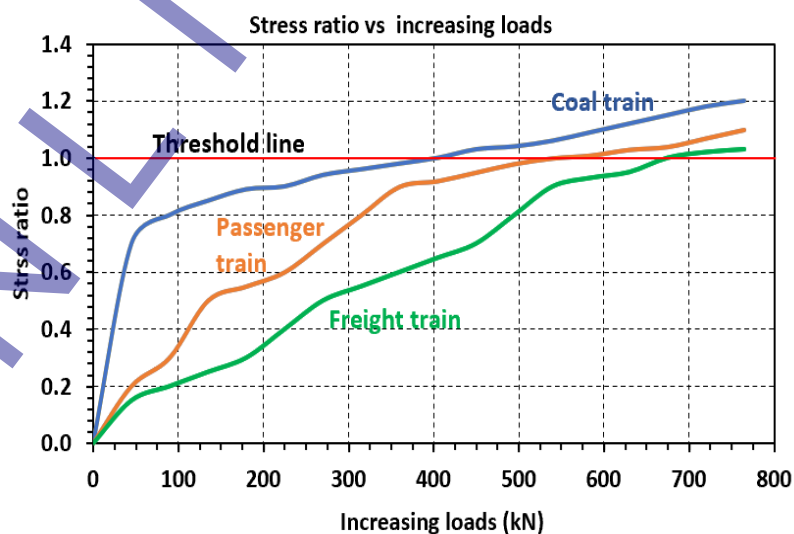


Fig. 11. Results of numerical simulation for Influence of increasing dynamic loads to stress ratio

3.5 Possibility of Double Resonance

It could be understood that if the natural frequency of a building structure indicates an equivalence value with a natural frequency of the surrounding environment, this condition may exhibit a potentially double resonance case [38]. Resonance on the railway bridge is a significant aspect that must be resolved and is a primary concern.

Resonance may reduce riding comfort, especially for high-speed trains. Structurally, the steel railway bridge resonance minimizes the strength of the bridge girder [39].

The natural frequency of the railway bridge was evaluated numerically using 2D finite element analysis. The study concerning the natural frequency of steel railway bridges at the same designated location was performed [40]. The natural frequency of the steel railway bridge and natural frequency on-site around the steel railway bridge were determined employing the microtremor data. The implication of the research study indicated that the object of the railway bridge would possibly experience a double resonance case. Even though other methods are necessary for validation of the finding results, resonance characteristics of a railway bridge could be influenced by moving loads of high-speed trains, damping ratios, and beam span length. It was reported that the resonance response of the two-span continuous beam and a simply supported beam is different. The two resonances are primarily caused by excitation frequencies that coincide generated by moving trains at various speeds. At the resonance condition, the more significant damping ratios lead to a smaller deflection [41].

All maximum dynamic moving loads applied on the railway bridge in Fig. 11 were selected for analyzing railway bridge frequencies. The maximum dynamic moving loads, and the harmonic frequency of the railway bridge exhibits similar tendency. For the maximum dynamic moving loads, it seems that the steel railway bridge resonance happens when the moving harmonic load is static and works on the steel railway bridge. It is understandable that the steel railway bridge vibrates due to dynamic moving loads with resonant velocity. No resonance might take place because the forces transverse to the railway bridge at a finite time [42]. Therefore, the maximum of the steel railway bridge response will not happen at the resonant velocity. Besides, the resonance is the maximum vibration response.

Moving loads and moving masses can complicate the determination of the dynamic response of steel railway bridges. This phenomenon happened because of the involvement of the moving loads and moving masses when the train passes over the railway bridge. According to the critical speed and resonance criteria [43], critical speed reduces when the amount of moving mass increases. Resonance severity is governed by the ratio between the bridge length and carriage length.

It was noticed that the occurrence of resonant speed is caused by the bridge and train parameters. The resonant speeds are reflected in the cumulative increase due to dynamic response. As the load increases, the deflection amplitude increases for the force that moves along the bridge passing through the beam. This is particularly dangerous for high-speed trains and has an adverse effect on the degradation of the superstructure as well as the fatigued bridge [44]. However, the moving load spectrum can be used to evaluate the bridge-free vibration extreme response [45].

4 CONCLUSIONS

In this work, a steel railway bridge structure with 61.60 meters in span length was studied to understand the behavior of the railway bridge under dynamic moving loadings. Three-dimensional numerical models of the steel railway bridge were developed. This study used the finite element technique for the numerical simulation of the steel railway bridge. In this regard, the various railway bridge parameters were thoroughly evaluated so as to determine threshold values of parameters, and severity levels have been developed to assess the serviceability of the railway bridge.

Further, the study revealed that the maximum deflection under critical dynamic moving loads calculated was 27.60 mm. The most crucial deformation of the steel railway bridge is when the coal train (Babaranjang train) passes over the railway bridge. Although the maximum deformation calculated is smaller than the maximum deformation recorded by the displacement sensors, the coal train (Babaranjang train) with a load of more than 450 kN is not permitted to pass through the bridge. Because when a coal train (Babaranjang train) with dynamic moving loads of more than 450 kN passes through a railway bridge, the stress ratio that occurs on the railway bridge will exceed the threshold, and the bridge has the potential to fail.

The determination of the safety level of the railway bridge is indicated by not exceeding the parameter value against the threshold criteria. Based on the boundary of the lower limit and upper limit of the natural frequency, the natural frequency of the railway bridge under study was 2.056 Hz and 4.345 Hz, respectively. Under the maximum dynamic moving load, the frequency of the railway bridge decreases with the passage of the period. The calculated frequency is included in the threshold criteria. Therefore, it seems that the maximum railway bridge response will not occur at the resonant velocity. The railway bridge resonance might take place when the moving harmonic load is in static condition and works on the steel railway bridge.

The possibility of steel railway bridge failure was detected when the stress ratio of the railway structure passed a value of one. The failure can be assessed numerically by simulating an increasing dynamic moving load applied to the railway bridge structure. There was an indication that the coal train (Babaranjang train) is the train with the most critical tendency to cause failure. When the additional loads on the coal train (Babaranjang train) reached 400 kN, the steel railway bridge was indicated to have failed.

5 ACKNOWLEDGEMENT

This paper is part of the study carried out in the Research Center for Transportation Technology (PR TT), National Research and Innovation Agency – BRIN, Jakarta, Indonesia, and the Civil Engineering Department of Sumatera Institute of Technology (ITERA). BRIN financed the study via National Research Budget, Research and Innovation

for Advanced Indonesia scheme and LPDP grants. The authors would like to express their gratitude for the financial support received from the institutions. The authors would also be grateful to reviewers who provided constructive suggestions.

The authors declare that there is no conflict of interest regarding the publication of this article. The authors confirmed that the paper is free of plagiarism.

All authors of this manuscript are main contributors and have an equal primary role in conducting research according to their fields of expertise and publishing this article in highly reputable and globally indexed journals.

6 REFERENCES

- [1] Barasa, W., Fiantika, T., Purnomo, D. A., and Aspar, W. A. N., (2020). The comparative study of railway bridge design load between PM 60/2012 and EN 1991: 2-2003. *Majalah Ilmiah Pengkajian Industri*. Vol. 14, no. 2, pp. 107-116, <https://doi.org/10.29122/mipi.v14i2.4196>.
- [2] Duvnjak, I., Damjanović, D., Bartolac, M., Frančić Smrkić, M., and Skender, A., (2019). Monitoring and diagnostic load testing of a damaged railway bridge. *Frontiers in Built Environment*. vol. 5, no. 108, pp. 1-11, <https://doi.org/10.3389/fbuil.2019.00108>.
- [3] Yunus, M. Z. M., Ibrahim, N., and Ahmad, F. S., (2018). A review on bridge dynamic displacement monitoring using global positioning system and accelerometer, *AIP Conference Proceedings* 1930. 020039-6, vol. 1930, issue 1, <https://doi.org/10.1063/1.5022933>.
- [4] Lee, S. C., Tee, B. P., Chong, M. F., Ku Mahamud, K. M. S., and Mohamad, H., (2019). Structural assessment for an old steel railway bridge under static and dynamic loads using fibre optic sensors, *International Conference on Smart Infrastructure and Construction 2019 (ICSIC): Driving data-informed decision-making*, (ICE Virtual Library Publishing), pp. 729-736, <https://doi.org/10.1680/icsic.64669.729>.
- [5] Zhu, J., and Zhang, Y., (2019). Damage detection in bridge structures under moving vehicle loads using delay vector variance method. *Journal of Performance of Constructed Facilities*. ASCE., vol. 33, no. 5, 040190049, [https://doi.org/10.1061/\(ASCE\)CF.1943-5509.0001314](https://doi.org/10.1061/(ASCE)CF.1943-5509.0001314).
- [6] Chilamkuri, K., and Kone, V., (2020). Monitoring of varadhi road bridge using accelerometer sensor. *Materials today: Proceedings*. vol. 33, no. 1, pp. 367-371, (Elsevier - ScienceDirect), <https://doi.org/10.1016/j.matpr.2020.04.159>.
- [7] Barasa, W., Aspar, W. A. N., Purnomo, D. A., Nadi, M. A. B., Fiantika, T., and Primadiyanti, S. P., (2023). Assessment of an existing steel railway bridge structure, July 21, 2023, *AIP Conference Proceedings* 2689, 040019 (2023), AIP Publication LLC, Melville, NY., USA., <https://doi.org/10.1063/5.0116333>.
- [8] Fiantika, T., Aspar, W. A. N., Purnomo, D. A., Barasa, W., Harjono, M. S., and Primadiyanti, S. P., (2023). A review of structural health monitoring systems and application for railway bridges. *AIP Conference Proceedings* 2646, 050006 (2023). AIP Publication LLC, Melville, NY., USA., <https://doi.org/10.1063/5.0115843>.
- [9] Purnomo, D. A., Aspar, W. A. N., Barasa, W., Harjono, M. S., Sukamdo, P., and Fiantika, T., (2021). Initial implementation of structural health monitoring system of a railway bridge. *The 2nd Global Congress on Construction Materials and Structure Engineering (2nd GCOMSE 2021)*, IOP Conference Series: Material Science and Engineering, 26–27 August 2021, Melaka, Malaysia, doi:10.1088/1757-899X/1200/1/012019.
- [10] Yue, L., and Zhang, K., (2021). Structural damage identification based on dynamic deflection sensitivity of bridge under vehicle loading. *Journal of Physics: Conference Series*, vol. 1846, 012002, IOP Publishing, doi:10.1088/1742-6596/1846/1/012002.
- [11] Shahsavari, V., Mehrkash, M., and Santini-Bell, E., (2020). Damage detection and decreased load-carrying capacity assessment of a vertical-lift steel truss bridge. *Journal of Performance of Constructed Facilities*. ASCE, vol. 34, no. 2, 04019123 (2020), [https://doi.org/10.1061/\(ASCE\)CF.1943-5509.0001400](https://doi.org/10.1061/(ASCE)CF.1943-5509.0001400).
- [12] Wang, Y., Wang, P., Tang, H., Liu, X., Xu, J., Xiao, J., and Wu, J., (2021). Assessment and prediction of high speed railway bridge long-term deformation based on track geometry inspection big data. *Mechanical System and Signal Processing*. Vol. 158, no. 10774, (ScienceDirect), <https://doi.org/10.1016/j.ymsp.2021.107749>.
- [13] *CSI Analysis Reference Manual for SAP2000*, (2016). *Integrated Finite Elements Analysis and Design of Structures tutorial Manual*, (Computers and Struct. Inc. (CSI), Berkeley, CA, USA), available at <https://docs.csiamerica.com/manuals/sap2000/CSiRefer.pdf>.
- [14] Larasati, M., Pariatmono, Fitriansyah, E. R., Amin, M., Muin, R. B., Suseno, D. A., Harjono, M. S., Purnomo, D. A., Aspar, W. A. N., Fiantika, T., and Pasadena, E. I. N. S. P. J. D. S., (2022). Measurement of geometric variations of a railway truss bridge (case study: bh77 railway bridge). *Majalah Ilmiah Pengkajian Industri*, vol. 16, no. 1, pp. 18-23, <https://doi.org/10.29122/mipi.v16i1.5177>.
- [15] Transportation Minister of the Republic of Indonesia (2012) Regulation no. 60 of 2012: *Railroad Technical Requirements* (Jakarta: Minister of Transportation), available at <https://djka.dephub.go.id/regulasi?lang=en>.

- [16] Barasa, W., Aspar, W. A. N., Sukamdo, P., Purnomo, D. A., Harjono, M. S., Nadi, M. A. B., and Adibroto, A., (2023). Monitoring displacement, strain, and acceleration of a steel railway bridge, *Ain Shams Engineering Journal*. Vol. 14, no. 11, October 15, 2023, article number 102521, <https://doi.org/10.1016/j.asej.2023.10521>.
- [17] Chen, Z., Zhou, X., Xu, W., Dong, L., and Qian, Y., (2017). Deployment of a smart structural health monitoring system for long-span arch bridge: A review and a case study. *MDPI Journal Sensor*, vol. 17, no. 9, 2151, doi:10.3390/s17092151.
- [18] Olaszek, P., Wyczałek, I., Sala, D., Kokot, M., and Swiercz, A., (2020). Monitoring of the static and dynamic displacements of railway bridges with the use of inertial sensors. *MDPI Journal Sensors*, vol. 20, no. 10, pp. 2767-2790, <http://dx.doi.org/10.3390/s20102767>.
- [19] Mohammed, A., Ambak, K., Mosa, A. M., and Syamsunur, D., (2019). Expert system in engineering transportation: A review. *Journal of Engineering Science and Technology*. vol. 14, no. 1, pp. 229–252, available at <https://www.researchgate.net/publication/331546229>.
- [20] Azim, M. R., and Gül, M., (2019). Damage detection of steel girder railway bridges utilizing operational vibration response. *Structural Control and Health Monitoring*. vol. 26, no. 11, e2447, <http://dx.doi.org/10.1002/stc.2447>.
- [21] Azim, M. R., and Gül, M., (2021). Development of a novel damage detection framework for truss railway bridges using operational acceleration and strain response. *MDPI Journal of Vibration*, vol. 4, no. 2, pp. 422–443, <https://doi.org/10.3390/vibration4020028>.
- [22] National Standardization of Indonesia, SNI 1725-2016, (2016). Indonesia National Standard: Loads for Bridges, (Jakarta: National Standardization of Indonesia), available at <https://akses-sni.bsn.go.id/sni>.
- [23] Jukowski, M., Bęc, J., and Zbiciak, A., (2021). Finite element analysis of train speed effect on dynamic response of steel bridge. *Open Engineering*. Vol. 11, issue 1, pp. 1122-1133, (De Gruyter), <https://doi.org/10.1515/eng-2021-0114>.
- [24] Gou, H., Ran, Z., Yang, L., Bao, Y., and Pu, Q., (2019). Mapping vertical bridge deformations to track geometry for high-speed railway. *Steel and Composite Structures*, vol. 32, no. 4, pp. 467-478, <https://doi.org/10.12989/scs.2019.32.4.467>.
- [25] Weichao, Y., Deng, E., Mingfeng, L., Zhihui, Z., and Pingping, Z., (2019). Transient aerodynamic performance of high-speed trains when passing through two windproof facilities under crosswinds: A comparative study. *Engineering Structures*. Vol. 188, pp. 729–44, <https://doi.org/10.1016/j.engstruct.2019.03.070>.
- [26] Deng, E., Weichao, Y., Deng, L., Zhihui, Z., Xuhui, H., and Ang, W., (2020). Time-resolved aerodynamic loads on high-speed trains during running on a tunnel–bridge–tunnel infrastructure under crosswind. *Engineering Applications of Computational Fluid Mechanics*. vol. 14, no. 1, pp. 202–221, (Taylor and Francis), doi: 10.1080/19942060.2019.1705396.
- [27] Lipecki, T., Bęc, J., Flaga, A., and Bosak, G., (2013). Aerodynamic analysis of a sinusoidal footbridge for pedestrian and bicycle traffic. *Roads and Bridges*. Vol.12, no. 3, pp. 297–316, DOI: 10.7409/rabd.013.021.
- [28] Faulkner, K., Huseynov, F., Brownjohn, J., and Xu, Y., (2018). Deformation monitoring of a simply supported railway bridge under varying dynamic loads. *Open Research Exeter, 9th International Association for Bridge Maintenance and Safety (IABMAS), Maintenance, Safety, Risk, Management and Life-Cycle Performance of Bridges, 1st ed.*, (Taylor & Francis Group), <http://dx.doi.org/10.1201/9781315189390-202>, also available at <http://hdl.handle.net/10871/35507>.
- [29] Zhu, Z., Tang, Y., Ba, Z., Wang, K., and Gong, W., (2022). Seismic analysis of high-speed railway irregular bridge–track system considering V-shaped canyon effect. *Railway Engineering Science*. vol. 30, pp. 57-70, <https://doi.org/10.1007/s40534-021-00262-x>.
- [30] Nadi, M. A. B., and Fauzan, S. A., (2019). Analysis image-based automated 3D crack detection for post-disaster bridge assessment in flyover Mall Boemi Kedaton. *Journal of Science and Applicative Technology*. Vol. 2, no. 1, pp. 2581-0545. <https://doi.org/10.35472/281449>.
- [31] National Standardization of Indonesia, SNI 1729-2015, (2015). Indonesia National Standard: Specifications for structural steel buildings, (Jakarta: National Standardization of Indonesia), available at <https://akses-sni.bsn.go.id/sni>.
- [32] European Standard 1991:2. (2003). Traffic Loads on Bridge, (European Committee for Standardization, Brussels, Belgium).
- [33] Azim, M. R., Zhang, H., and Gül, M., (2020). Damage detection of railway bridges using operational vibration data: theory and experimental verifications. *Structural Monitoring and Maintenance*. vol. 7, issue 2, pp. 149–166, <https://doi.org/10.12989/smm.2020.7.2.149>.
- [34] Azim, M. R., and Gül, M., (2020). Damage detection of steel-truss railway bridges using operational vibration data. *Journal of Structural Engineering ASCE*, vol. 146, no. 3, 04020008 (2020), [http://dx.doi.org/10.1061/\(ASCE\)ST.1943-541X.0002547](http://dx.doi.org/10.1061/(ASCE)ST.1943-541X.0002547).

- [35] Azim, M. R., and Gül, M., (2021). Data-driven damage identification technique for steel truss railroad bridges utilizing principal component analysis of strain response. *Structure and Infrastructure Engineering*. vol. 17, no. 8, pp. 1019-1035, Taylor & Francis Online, <http://dx.doi.org/10.1080/15732479.2020.1785512>.
- [36] Azim, M. R., and Gül, M., (2020). Damage detection framework for truss railway bridges utilizing statistical analysis of operational strain response. *Structural Control and Health Monitoring*. Vol. 27, issue 8, e2573, <http://dx.doi.org/10.1002/stc.2573>.
- [37] Zhang, H., Gül, M., and Kostic, B., (2019). Eliminating temperature effects in damage detection for civil infrastructure using time series analysis and autoassociative neural networks. *Journal of Aerospace Engineering*. ASCE. Vol. 32, no. 2, (2019) 04019001, [http://dx.doi.org/10.1061/\(ASCE\)AS.1943-5525.0000987](http://dx.doi.org/10.1061/(ASCE)AS.1943-5525.0000987).
- [38] Billah, K. Y., and Scanlan, R. H., (1991). Resonance, Tacoma Narrows Bridge failure, and undergraduate physics textbooks. *American Journal of Physics*. vol. 59, no. 2, pp. 118-124, <https://doi.org/10.1119/1.16590>.
- [39] Matsuoka, K., Tanaka, H., Kawasaki, K. I., Somaschini, C., and Collina, A., (2021). Drive-by methodology to identify resonant bridges using track irregularity measured by high-speed trains. *Mechanical System and Signal Processing*. Vol. 158, no. 107667, <https://doi.org/10.1016/j.ymssp.2021.107667>.
- [40] Nadi, M. A. B., Nurfaizia, Karunia, M. N., Aspar, W. A. N., Barasa, W., Fudholi, A., (2022). Characterization of site effect and natural frequency of railway bridges. *International Journal of Sustainable Development and Planning*. Vol. 17, no. 1, pp. 243-249, <https://doi.org/10.18280/ijstdp.170124>.
- [41] Wang, Y., Weia, Q.-C., Shi, J., and Long, X., (2010). Resonance characteristics of two-span continuous beam under moving high speed trains. *Latin American Journal of Solids and Structures*. vol. 7, no. 2, pp. 185-199, <http://dx.doi.org/10.1590/S1679-78252010000200005>.
- [42] Pesterev, A. V., Yang, B., Bergman, L. A., and Tan, C. A., (2003). Revisiting the moving force problem. *Journal of Sound and Vibration*, vol. 261, no. 1, pp. 75–91, [https://doi.org/10.1016/S0022-460X\(02\)00942-2](https://doi.org/10.1016/S0022-460X(02)00942-2).
- [43] Mao, L., and Lu, Y., (2013). Critical speed and resonance criteria of railway bridge response to moving trains. *Journal of Bridge Engineering*. ASCE, vol. 18, no. 2, pp. 131-141, [http://dx.doi.org/10.1061/\(ASCE\)BE.1943-5592.0000336](http://dx.doi.org/10.1061/(ASCE)BE.1943-5592.0000336).
- [44] Moravčík, M. and Moravčík, M., (2017). Dynamic response of railway bridges subjects to passing vehicles. *Transactions of the VŠB – Technical University of Ostrava, Civil Engineering Series*, vol. 17, no. 2, pp. 79-88, <http://dx.doi.org/10.1515/tvsb-2017-0031>.
- [45] Li, J., and Zhang, H., (2020). Moving load spectrum for analyzing the extreme response of bridge free vibration. *Shock and Vibration*, vol. 2020, ID 9431620, pp. 1-13, <https://doi.org/10.1155/2020/9431620>.

Paper submitted: 22.06.2023.

Paper accepted: 21.03.2024.

This is an open access article distributed under the CC BY 4.0 terms and conditions

ONLY